ISSN 1392 - 1207. MECHANIKA. 2006. Nr.2(58)

Multi layer tubular composite reinforced by a liner: behaviour under thermo mechanical loading simulation

A. Hocine*, A. Bezazi, A. Benamar***, L. Boubakar****, A. Kondratas*******

**University Hassiba Benbouali of Chlef BP. 151, Chlef 02000, Algeria, E-mail: Hocinea_dz@Yahoo.fr*

***University 08 Mai 1945, BP. 401, Guelma 24000, Algeria, E-mail: ar_bezazi@yahoo.com*

**** ENSET, Department of mechanical engineering, BP 1523, Oran 31000, Algeria, E-mail: benamar_dz@yahoo.fr*

***** University of Franche-Comté, LMARC, 24, chemin de l'Epitaphe, 25000 Besançon, France, E-mail: lamine.boubakar@univ-fcomte.fr*

******Kaunas University of Technology, Donelaicio str. 73, 44029, Kaunas, Lithuania, E-mail: Alvydas.Kondratas@ktu.lt*

1. Introduction

The principal responsible for the change of the atmosphere's average temperature is the carbon dioxide counting for about 53% of the additional greenhouse effect. In addition to this environmental concern, the overuse of the world's reserves of fossilized fuel is also a source of apprehension. The consumption of the most significant energy is superior in residential areas as well as services and transport sectors. It appears that these sectors are to be supplied with fossil, nuclear, and renewable energy, such as: electricity (a fuel without carbon) and hydrogen (a hydrocarbon or an alcohol resulting from the biomass). The biomass is used partially in automobile fuel with a great potential, however, it is only a small proportion given the huge demand. Taking into account the constraints related to electricity transmission, one can reasonably think that it can only support a part of the expected increase. Hydrogen sources can be various and their similarities with natural gas are large in terms of the chain of storage, transport, and use. It will be the future solution which can replace the classical energy sources and preserves the greenhouse [1]. At present, there are three types of storage of hydrogen [2].

- Liquefied hydrogen. This technique makes possible to have a higher volume and a better gravimetric density than the other techniques. However, a great quantity of gas is required to liquefy hydrogen, as well as a special reserve of storage with an effective layer of heat insulation. The latter will allow reducing the evaporation of hydrogen over a long duration.
- Compressed hydrogen gas. This technique is characterized by a very simple system of storage and a better transport and storage cost compared to the other techniques. However, this technique allows only the storage of small volume density.
- Hydrogen storage in the hydrides. An old technique of storage, hence it is very secure and completely controllable. Nevertheless, this storage mode has two defects: the hydrides are heavy and their storage capacity is low.

Hydrogen poses two problems of storage: on one hand it weakens several materials; and on the other, because of its small size, it diffuses through the tanks. For this reason, the first tanks were manufactured from steel or aluminium alloys etc; which are, unfortunately, too heavy for a car [3]. Indeed, the tanks are currently made out of composite materials, which are characterized by their lightlightness, rigidity, good fatigue strength and the absence of corrosion when their components are not metallic etc [4, 5]. Several models of hydrogen storage were proposed to resolve these problems. A model of hydrogen storage which combined between a light tank at high pressure and an alloy of storage was proposed [2]. The liner prevents hydrogen from escaping and the composite rolling up must resist the high gas pressures. The hybrid approach ensures a perfect participation between the liner and the composite hull, as well as the use of the totality of resistance in tension of the composite. The choice of the liner is important when designing a composite tank for gas storage at high pressure. The aim of this choice is to prevent the diffusion through the wall or when it is conceived for storing liquids subjected to temperature variations [6]. At Technological conference of energy in TEXAS (1977th), researchers came up with a tank with several types of liners. Generally, they can be grouped in three different types of liner [6].

- Elastomer. They are applicable when load can not be supported, at temperatures close to ambient and with tolerable permeability.
- Thin liner. This type of liner does not contribute to the capacity of the loads supported by the tank and it exhibits other problems, such as: buckling during the phase of decompression and the difficulties during manufacturing.
- Thick liner. The use of this type allows supporting up to 1/3 of the load of the tank internal pressure.

The study of the multi layer tank behaviours was investigated by several researchers; few of them have used an analytical approach. An analytical base for the research and the analysis of the mechanical properties of a multilayer tube under thermo mechanical loading was provided by [7, 8]. A procedure for the design and the prediction of the behaviour of a tank under pressure combining between the mechanical and hydrothermal effect was analytically developed [9]. The different types of loads, such as: the internal pressure, the axial load, the load of the mass due to rotation by adding the temperature, and the variation of humidity through the body were considered. The classical theory of the laminates and the model of the generalized plane deformation were used for the formulation of the elastic problem. Due to the axisymmetry of the loading, the problem is simplified to a function of stress depending only on radial coordinate of the cylinder.

In the case of reinforcement by a liner, the bursting pressure of a composite carbon fibre tank or Kevlar

coated with a metallic liner was calculated. Also, the effects of the thickness variation and the orientation of the layers on the pressure of bursting were discussed. The determination of the adequate stacking sequence allowing improving resistance of the cylindrical composite laminated glass/epoxy tanks subjected to internal and external pressures was investigated [10-12]. The modeling was made by the use of a computer code, based on structured method known as "Blocks". The results of the modeling were adapted in the SAP90 software, where a data file was prepared.

This work represents the continuation of the investigation of the multilayer tubular composite reinforced by a liner behaviour under pressure loading. It allows the study of the thermo-mechanical behaviour of a multilayer composite tube reinforced by an aluminum liner. A thermo mechanical comparative study between the quasi-isotropic laminate [liner/±60/$(90)_2$] and the antisymmetric one [liner/$(\pm 60)_2$] was established. These laminates were chosen since they gave good behaviour when subjected to a mechanical loading. It should be noticed that the two stacking sequences were subjected to an internal pressure of 25.8 MPa compared to 10 MPa used in [13].

2. Analysis procedure

2.1. Stress and strain analysis

A multilayer cylindrical tube reinforced by a liner of internal and external radius r_0 and r_a respectively, subjected to a thermomechanical loading was consider. The coordinates of the cylinder, r radial, θ circumferential and z axial as defined [13]. Stress displacement relations for layer k, for anisotropic materials are given by [14]

$$\begin{Bmatrix}\sigma_z\\ \sigma_\theta\\ \sigma_r\\ \tau_{\theta r}\\ \tau_{zr}\\ \tau_{z\theta}\end{Bmatrix}^{(k)} = \begin{bmatrix}\boldsymbol{C}_{11} & \boldsymbol{C}_{12} & \boldsymbol{C}_{13} & 0 & 0 & \boldsymbol{C}_{16}\\ \boldsymbol{C}_{12} & \boldsymbol{C}_{22} & \boldsymbol{C}_{23} & 0 & 0 & \boldsymbol{C}_{26}\\ \boldsymbol{C}_{13} & \boldsymbol{C}_{23} & \boldsymbol{C}_{33} & 0 & 0 & \boldsymbol{C}_{36}\\ 0 & 0 & 0 & \boldsymbol{C}_{44} & \boldsymbol{C}_{45} & 0\\ 0 & 0 & 0 & \boldsymbol{C}_{45} & \boldsymbol{C}_{55} & 0\\ \boldsymbol{C}_{16} & \boldsymbol{C}_{26} & \boldsymbol{C}_{36} & 0 & 0 & \boldsymbol{C}_{66}\end{bmatrix}^{(k)} \times$$

$$\times \begin{Bmatrix}\varepsilon_z - \alpha_z \Delta T\\ \varepsilon_\theta - \alpha_\theta \Delta T\\ \varepsilon_r - \alpha_r \Delta T\\ \gamma_{\theta r}\\ \gamma_{zr}\\ \gamma_{z\theta} - \alpha_{z\theta} \Delta T\end{Bmatrix}^{(k)} \qquad (1)$$

where σ_z, σ_θ, and σ_r are the axial, circumferential, and radial stress vectors respectively; $\tau_{z\theta}$, τ_{zr}, and $\tau_{\theta r}$ are the shear stress vectors in the planes z-θ, z-r, θ-r respectively; k is the number of the respective layer; $\boldsymbol{C}_{11}$-$\boldsymbol{C}_{66}$ are the rigidity coefficients matrices of the respective layer, $\boldsymbol{\varepsilon}_z$, $\boldsymbol{\varepsilon}_\theta$, and $\boldsymbol{\varepsilon}_r$ are the axial, circumferential, and radial strain vectors respectively; $\boldsymbol{\gamma}_{\theta r}$, $\boldsymbol{\gamma}_{zr}$, and $\boldsymbol{\gamma}_{z\theta}$ are the shear strain vector in the plane θ-r, z-r, and z-θ respectively; α_z α_θ α_r, and $\alpha_{z\theta}$ are the thermal coefficients, expressed in the reference mark of the cylinder (r, θ, z); ΔT is the difference in temperature. For the multilayer these coefficients are determined by the following expression [15]

$$\{\overline{\alpha}\} = [T_\varepsilon]\{\alpha\}$$

or

$$\begin{Bmatrix}\alpha_z\\ \alpha_\theta\\ \alpha_r\\ \alpha_{z\theta}\end{Bmatrix}^{(k)} = \begin{bmatrix} m^2 & n^2 & mn\\ n^2 & m^2 & -mn\\ 1 & 0 & 0\\ -2mn & 2mn & m^2-n^2\end{bmatrix}^{(k)} \begin{Bmatrix}\alpha_X\\ \alpha_Y\\ \alpha_Y\end{Bmatrix}^{(k)} \qquad (2)$$

where $m = cos\,\varphi$, $n = sin\,\varphi$, α_X and α_Y are the thermal coefficients of single layer, in the material's main axis (L-T) which are longitudinal and the transverse principal axes of the fibre respectively.

According to the context of the axisymmetry, the relation deformations/displacements can be written in the following form [13]

$$\begin{aligned}&\frac{d\sigma_r^{(k)}}{dr} + \frac{\sigma_r^{(k)} - \sigma_\theta^{(k)}}{r} = 0\\ &\frac{d\tau_{\theta r}^{(k)}}{dr} + \frac{2}{r}\tau_{\theta r}^{(k)} = 0\\ &\frac{d\tau_{zr}^{(k)}}{dr} + \frac{\tau_{zr}^{(k)}}{r} = 0\end{aligned} \qquad (3)$$

The relation deformations/displacements can be also reduced [13]

$$\begin{aligned}&\varepsilon_r^{(k)} = \frac{dU_r^{(k)}}{dr} \;;\; \varepsilon_\theta^{(k)} = \frac{U_r^{(k)}}{r} \;;\; \varepsilon_z^{(k)} = \frac{dU_z^{(k)}}{dz} = \varepsilon_0\\ &\gamma_{zr}^{(k)} = 0 \;;\; \gamma_{\theta r}^{(k)} = \frac{dU_\theta^{(k)}}{dr} - \frac{U_\theta^{(k)}}{r}\\ &\gamma_{z\theta}^{(k)} = \frac{dU_\theta^{(k)}}{dz} = \gamma_0 r\end{aligned} \qquad (4)$$

2.2. Metallic liner behaviour

The elastic tensor of rigidity in the cylindrical reference mark of the tank can be written in the following form [14]

$$\boldsymbol{C}_l = \begin{bmatrix}\boldsymbol{C}_{11} & \boldsymbol{C}_{12} & \boldsymbol{C}_{12} & 0 & 0 & 0\\ \boldsymbol{C}_{12} & \boldsymbol{C}_{11} & \boldsymbol{C}_{12} & 0 & 0 & 0\\ \boldsymbol{C}_{12} & \boldsymbol{C}_{12} & \boldsymbol{C}_{11} & 0 & 0 & 0\\ 0 & 0 & 0 & \boldsymbol{C}_{66} & 0 & 0\\ 0 & 0 & 0 & 0 & \boldsymbol{C}_{66} & 0\\ 0 & 0 & 0 & 0 & 0 & \boldsymbol{C}_{66}\end{bmatrix} \qquad (5)$$

where $\boldsymbol{C}_l$ is the rigidity matrix of the metal liner.

2.3. Behaviour of the multilayer composite

The rigidity matrix of the composite laminate is written in the following form [14].

The rigidity matrix $\boldsymbol{C}$ of the tube composite/liner is expressed as follows

- $\boldsymbol{C} = \boldsymbol{C}_l$ for $k = 1$
  $\boldsymbol{C} = \boldsymbol{C}_c$ for $k \neq 1$.

2.4. Formulation of the problem

Substituting Eq. (1) in (3) and using (4), the following differential equation is obtained

$$\frac{d^2U_r^{(k)}}{dr^2} + \frac{1}{r}\frac{dU_r^{(k)}}{dr} - \frac{N_1^{(k)}}{r^2}U_r^{(k)} = \\ = [N_2^{(k)}\,\varepsilon_0 + N_3^{(k)}\,\Delta T]\frac{1}{r} + N_4^{(k)}\,\gamma_0 \qquad (7)$$

where $U_r^{(k)}$ is radial displacement of the layer k and

$$N_1^{(k)} = \beta^{(k)};\ N_2^{(k)} = \frac{\boldsymbol{C}_{12}{}^{(k)} - \boldsymbol{C}_{13}{}^{(k)}}{\boldsymbol{C}_{33}{}^{(k)}};$$
$$N_3^{(k)} = \frac{K_3{}^{(k)} - K_2{}^{(k)}}{\boldsymbol{C}_{33}{}^{(k)}};\ N_4^{(k)} = \frac{\boldsymbol{C}_{26}{}^{(k)} - \boldsymbol{C}_{36}{}^{(k)}}{\boldsymbol{C}_{33}{}^{(k)}};$$
$$K_2^{(k)} = \boldsymbol{C}_{12}^{(k)}\alpha_z^{(k)} + \boldsymbol{C}_{22}^{(k)}\alpha_\theta^{(k)} + \boldsymbol{C}_{23}^{(k)}\alpha_r^{(k)} + \boldsymbol{C}_{26}^{(k)}\alpha_{z\theta}^{(k)};$$
$$K_3^{(k)} = \boldsymbol{C}_{13}^{(k)}\alpha_z^{(k)} + \boldsymbol{C}_{23}^{(k)}\alpha_\theta^{(k)} + \boldsymbol{C}_{33}^{(k)}\alpha_r^{(k)} + \boldsymbol{C}_{36}^{(k)}\alpha_{z\theta}^{(k)}$$

For an anisotropic material

$$\boldsymbol{C}_{22}{}^{(k)}\big/\boldsymbol{C}_{33}{}^{(k)} > 0\ ;\ \boldsymbol{C}_{22}{}^{(k)}\big/\boldsymbol{C}_{33}{}^{(k)} \neq 1 \qquad (8)$$

By letting $\beta^{(k)} = \sqrt{\boldsymbol{C}_{22}{}^{(k)}\big/\boldsymbol{C}_{33}{}^{(k)}}$ the solution of equation (7) takes the following form:

if $\beta^{(k)} = 1$, then

$$U_r^{(k)} = D^{(k)}r + J^{(k)}/r + \\ + r\,ln(r)\left(N_2^{(k)}\,\varepsilon_0 + N_3^{(k)}\,\Delta T\right) + \alpha_4^{(k)}\,\gamma_0\,r^2 \qquad (9)$$

if $\beta^{(k)} \neq 1$, then

$$U_r{}^{(k)} = D^{(k)}r^{\beta^{(k)}} + J^{(k)}r^{-\beta^{(k)}} + \\ + \left(\alpha_2^{(k)}\,\varepsilon_0 + \alpha_3^{(k)}\,\Delta T\right)r + \alpha_4^{(k)}\,\gamma_0\,r^2 \qquad (10)$$

with

$$\alpha_2^{(k)} = \frac{N_2^{(k)}}{1 - N_1^{(k)}};\ \alpha_3^{(k)} = \frac{N_3^{(k)}}{1 - N_1^{(k)}};\ \alpha_4^{(k)} = \frac{N_4^{(k)}}{1 - N_1^{(k)}} \qquad (11)$$

where $D^{(k)}$ and $J^{(k)}$ are the integration constants.

2.5. Boundary conditions

The boundary conditions are imposed by the geometry conditions of the structure due to continuity and volume conservation, and by the conditions of loading. It is assumed that there are no slips in the interfaces and that there is a continuity of stresses and displacements. The boundary conditions are the same used in [13].

3. Algorithm of the procedure

The analytical resolution of the elastic behaviour of a multilayer tube reinforced by a metal liner under thermomechanical loading is solved using MATLAB software. In this analysis, all the structure of the tank is constituted of four composite carbon/epoxy layers. The analysis includes a comparative study between two types of laminates: the quasi-isotropic $[\pm\varphi_n/90_{2n}]$, and the multilayer antisymmetric $[\pm\varphi_{2n}]$, where φ =60° and n=1.

The stacking sequence of the studied laminates are [liner/±60/$(90)_2$] and [liner/$[(\pm60)_2$] corresponding to Seq1 and Seq2 respectively.

The objective of this analysis is to study the influence of the heating effect on the behaviour of the composite structure. Thus a comparative analysis is established between the results of this study (Seq1 and Seq2) and those of [13] (Seq3 and Seq6).

These laminates proved a good behaviour when subjected to a mechanical loading [13].

The considered tube is characterized by an internal radius of 50 mm, and 0.5 mm thickness of the liner and each layer of the composite. The elastic characteristics are given in [13] and the thermal properties of the two materials are presented in Table.

Table

Thermal characteristics

Properties	Carbon/Epoxy (T300/934) (10^{-6} K^{-1})	Aluminium Liner (10^{-6} K^{-1})
α_L	0.006	23.9
α_T	30.04	-

α_L and α_T are the thermal coefficients dilatation expressed in the reference mark of fibre *L-T*.

The internal wall of the composite tube is subjected to thermomechanical loads such as internal and external pressures of 25.8 and 1 MPa respectively, and a temperature of 100 K. The applied internal pressure was 10 MPa [13]. All results are represented as a function of a non-dimensional ratio R wich is expressed as

$$R = \frac{r - r_0}{r_a - r_0}$$

where r_0 and r_a are the internal and external radius of the multilayer tube respectively.

4. Results and discussions

4.1. Stresses

The distribution of the axial, circumferential, radial, and shear stresses σ_z, σ_θ, σ_r and $\tau_{z\theta}$ respectively through the wall's thickness is important in order to locate

the critical zones. The obtained results show that the stresses σ_z, σ_θ, and $\tau_{z\theta}$ exhibit a discontinuous variation as a function of R. In comparison to the results obtained in [13] with an internal pressure of 10 MPa, the results of this work have increased roughly with a factor of 2.5 which corresponds to the increases in the internal pressure. However, the behaviour of the stresses remained the same for both values of pressure.

Fig. 1 shows that the variation of the axial stress σ_z versus R is significantly different for the two types of the stacking sequences.

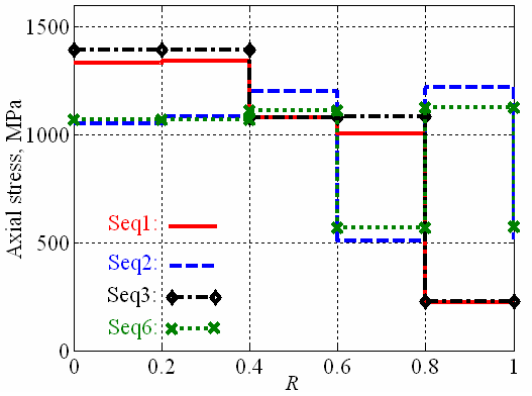

Fig. 1 Variations of the axial stress through the thickness

It can also be noticed that the change in the fibers orientation from one layer to another influences both the stress's behaviour and trend.

The stress σ_z variation for the sequence Seq1 $(\pm 60/90_2)$ is characterized by three stages: the first stage $(0 \le R \le 0.4)$ is characterized by the maximum stress of 1340 MPa; in the second one $(0.4 \le R \le 0.8)$, the stress drops slightly to the value of 1015 MPa, then it increases to 1075 MPa for $0.6 \le R \le 0.8$. In the final stage $(0.8 \le R \le 1)$ the stress drops sharply to reach the minimum of 225 MPa.

The stress distribution in the second sequence Seq2 $(\pm 60)_2$ is significantly different. It is characterized by three stages versus the ratio R: in the first stage for R=0 to 0.6 the axial stress takes the form of three small increments, reaching the maximum value in the third one 1040 MPa $(0.4 \le R \le 0.6)$, in the second stage $(0.6 \le R \le 0.8)$, σ_z drops sharply to the minimum value of 585 MPa, and in the third stage $(0.8 \le R \le 1)$ the stress increases sharply reaching the maximum again before dropping suddenly to the minimum value at the external wall.

The presence of the thermal effect in this work induced a slight decrease for $(0 \le R \le 0.6)$ in the axial stress for both sequences. No noticeable difference is noticed for the laminate Seq1 for $(0.6 \le R \le 1)$, whereas a minor increase is noticed for the laminate Seq2 for $(0.6 \le R \le 0.8)$, however a slight decrease is noticed for $(0.8 \le R \le 1)$.

The analyses show that the maximal axial stress is located at the inner wall of the cylinder for Seq1 whereas it is in the middle and just below the outer wall for Seq2.

Fig. 2 represents the variation of the circumferential stress σ_θ for the two stacking sequences as a function of the non-dimensional ratio R.

The stress distribution has the same trend, in the form of stairs, for both sequences, but differs in values. The values of σ_θ for Seq1 $(\pm 60/90_2)$ are significantly lower than those of Seq2 $(\pm 60°)_2$ up to R=0.4. How

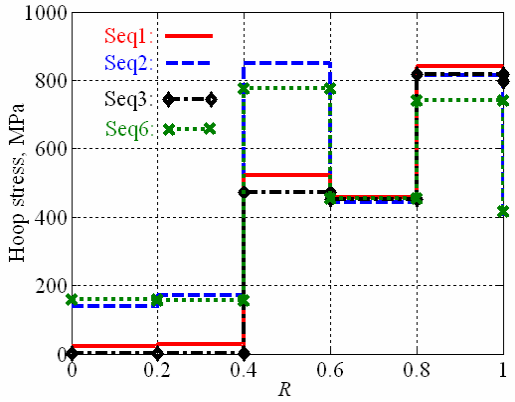

Fig. 2 Variations of the circumferential stress through the thickness

ever, the difference is negligible for $0.6 \le R \le 1$. Compared to axial stress, the thermal effect on the circumferential one is much more pronounced and causes an increase of the latter especially for $(0.4 \le R \le 1)$. In other words, the thermal effect induced an increase of the maximal stresses σ_θ , i.e. an increase of 13% for Seq2 for $(0.4 \le R \le 0.6)$ and 10% for Seq1 in the interval $(0.8 \le R \le 1)$. In addition the maximal effect is recorded with an increase of 33% and 18% for Seq2 and Seq1 respectively for $(0.6 \le R \le 0.8)$.

The thermal effect on the radial stress σ_r versus R is remarkable for $(0 \le R \le 0.2)$ (Fig. 3), where its presence induces a state of tension at the internal wall.

This state develops into compression while passing to the first composite layer, where the value of the radial stress is almost equal to the internal pressure of 25 MPa, for the two studied stacking sequences. However, the thermal effect is negligible for $(0.2 \le R \le 1)$. Seq2 is always the most affected compared to Seq1.

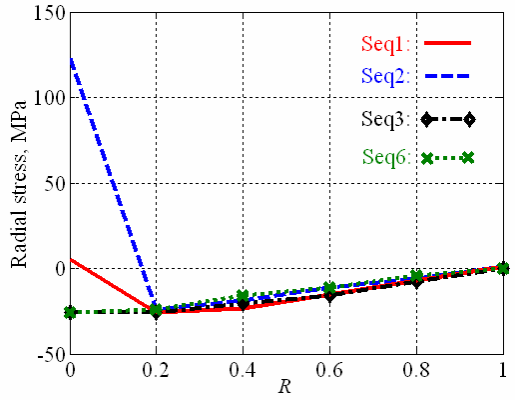

Fig. 3 Variations of the radial stress through the thickness

The variation of radial stress versus R for both stacking sequences has the same trend, i.e. varies linearly and occurs in two stages from the internal wall to the external one. The stress takes its maximum value at the internal wall with 113 MPa for Seq2 and 6 MPa for Seq1 in stage one $(0 \le R \le 0.2)$. The presence of the thermal effect allowed the increase of σ_r by 450% and 120% in the internal wall, for Seq2 and Seq1 respectively; and leads to the change from the state of compression stresses to the state

of tension stresses. Then it decreases sharply reaching a minimum value of -23 MPa for Seq2 and -25 for Seq1 for R=0.2. The radial stress starts increasing gradually reaching 1 MPa (external pressure) at the external wall R=1 in stage two ($0.2 \le R \le 1$). It should be noted that positive and negative values of stress correspond to tension and compression respectively.

For both sequences, the behaviour of the shear stress $\tau_{z\theta}$ versus R (Fig. 4) has the same trend, but differs in values and occurs in four stages starting from the internal wall to the external one: the shear stress is minimal (-20 and 163 MPa for Seq1 and Seq2) in the first stage for $0 \le R \le 0.4$ respectively, it reaches the maximum (870 and 985 MPa for Seq1 and Seq2) in the second stage for $0.4 \le R \le 0.6$ respectively, it drops to negative values in the

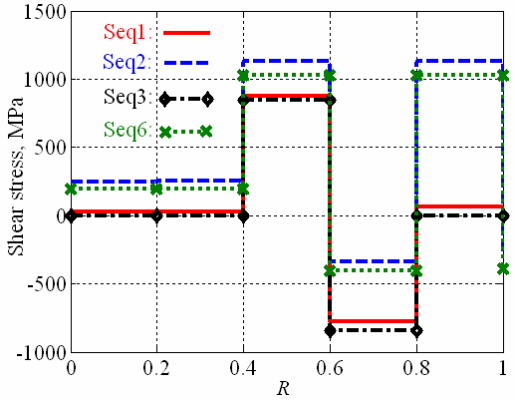

Fig. 4 Variations of the shear stress through the thickness

third stage for $0.6 \le R \le 0.8$, and, for Seq2, the shear stress becomes positive and takes the maximum value before decreasing again to the value of -447 MPa at the external wall in the forth stage for $0.8 \le R \le 1$, whereas for Seq1 the stress increases, yet a negative value, to -44 MPa.

The shear stress is less influenced by the presence of the thermal effect compared to the other stresses, where Seq2 remains the most sensitive than Seq1.

4.2. Strains

Figs. 5 - 8 indicate the variation of the axial, circumferential, radial, and shear strains through the thickness of the composite/liner tube for both sequences. These variations are linear either constant or with varying slope from one layer to another depending on the type of strain.

The axial strain through the thickness is constant (Fig. 5) and the values of Seq2 are lower than Seq1. The thermal effect has little influence on the axial strain, where it only decreases the values by 3% and 0.5% for Seq1 and Seq2 respectively.

Fig. 6 shows that the variation of the circumferential strains is linear with a changing slope and occurs in two stages: it remains constant at the first stage ($0 \le R \le 0.2$) and decreases at the second stage ($0.2 \le R \le 1$) to reach the minimum at the external wall. This time the values for Seq2 are larger than the ones of Seq1, and the higher the value of strain the more significant thermal effect is. The presence of the thermal effect decreased the hoop stress by 4% and 2% for Seq2 and Seq1 respectively.

The thermal effect on the radial strain has a similar trend to the radial stress, since at the internal wall an increase of over 26% is recorded for Seq2 and about 1.4% for Seq1, as shown in Fig. 7. The variation of the radial strain through the thickness has a similar trend for both

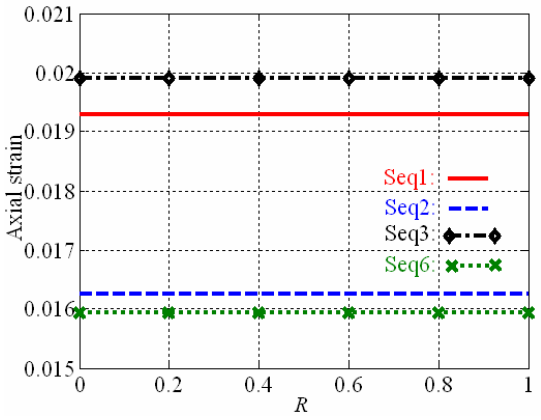

Fig. 5 Variations of the axial strain through the thickness

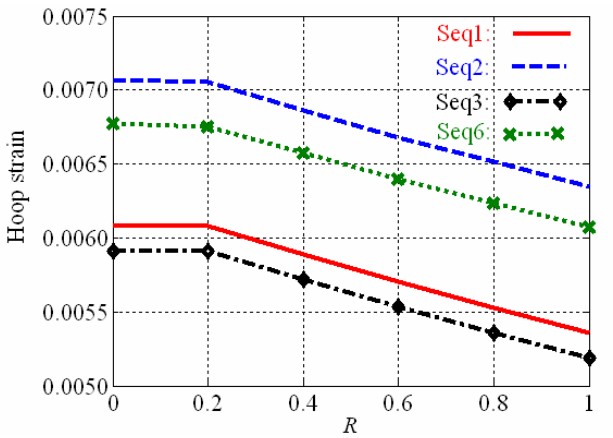

Fig. 6 Variations of the circumferential strain through the thickness

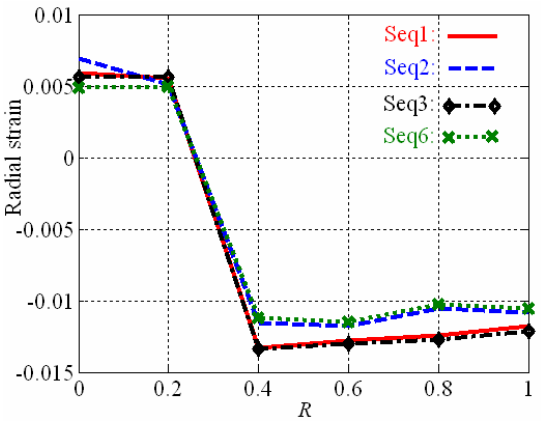

Fig. 7 Variations of the radial strain through the thickness

staking sequences and occurs in three stages: at the first stage ($0 \le R \le 0.2$) the radial strain decreases slightly before dropping sharply to reach a negative minimum value in the second stage ($0.2 \le R \le 0.4$). The radial strain increase slightly with yet a negative value in the third stage ($0.4 \le R \le 1.0$). Another observation is that the radial strain values of Seq1 are slightly lower than Seq2.

Fig. 8 shows a linear variation of the shear strain for Seq2 which increases slightly from the internal wall to

the external one; however, a constant shear strain is recorded for Seq1. Much larger values are obtained for Seq2 compared to Seq1. The thermal effect increased the shear strain for both stacking sequences, where the effect is more significant for Seq2 and lead to a negative shear strain for Seq1.

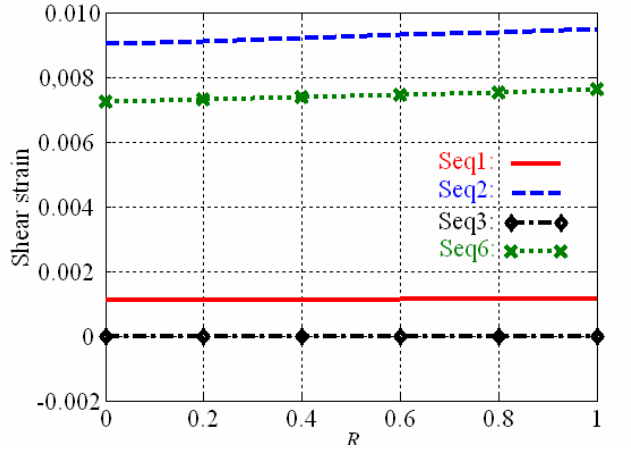

Fig. 8 Variations of the shear strain through the thickness

4.3. Displacement

The variation of radial displacements U_r for the two stacking sequences is shown in Fig. 9, where a similar trend is observed and the maximum displacements are recorded at the internal wall.

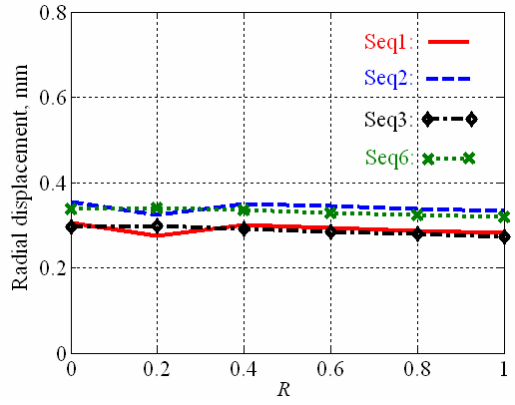

Fig. 9 Variations of the radial displacement through the thickness

Starting from the internal wall, this variation occurs in two stages: remain almost constant for $(0 \le R \le 0.2)$, and then it decreases gradually to the minimum value at the external wall for $(0.2 \le R \le 1)$.

The values of the radial displacement are larger for Seq2 compared to Seq1. The thermal effect in this case leads to an increase of the radial displacement for both stacking sequences, where the effect is more significant for Seq2 than for Seq1.

5. Conclusions

This investigation presented an analytical modelling of a multilayer composite cylindrical tank coated with an aluminium liner subjected to a thermomechanical loading. An elastic solution was presented for the quasi-isotropic laminate [liner/±60/$(90)_2$] and the antisymmetric one [liner/$(\pm60)_2$]. An analysis of stresses, strains, and displacement through the thickness was discussed and the presence of compression stresses on the internal wall and tension ones on the external wall of the composite tube was observed.

The presence of the thermal effect modifies the mechanical behaviour of the multilayer tube, i.e. either increases or decreases in terms of stresses, strains and displacements with different sensitivities. The thermal effect has a great influence at the internal wall where an increase in the radial stress by 450% and in the radial strain of over 26% has been recorded for Seq2. On the other hand, a slight increase or decrease was observed for the other stresses, strains, and displacements. In other words, the variation in the temperature produced a thermal dilation (extension or contraction) according to the sequence of stacking.

The stacking sequence $(\pm60/90_2)$ presents the best results in term of stresses and displacements compared to $[(\pm60)_2]$.

References

1. **Junker, M.**, **Bocquet, L.**, **Bendif, M.**, **Karboviac, D.** L'hydrogène pour le transport sur route -réalisations et développements. Ann. Chim. Sci. Mat, 2001, v.26(4), p.117-130.
2. **Takeichia, N.**, **Senoha, H.**, **Yokotab, T.**, **Tsurutab, H.**, **Hamadab, K.**, **Takeshitac, H. T.**, **Tanakaa, H.**, **Kiyobayashia, T.**, **Takanod, T.**, **Kuriyamaa, N.** Hybrid hydrogen storage vessel. A novel high pressure hydrogen storage vessel combined with hydrogen storage material.-Int. J. of Hydrogen Energy, 2003, v.28, p.1121-1129.
3. **Hocine, A.**, **Boubakar, L.**, **Bezazi, A.**, **Benamar, A.** Analyse d'un réservoir multicouche de stockage d'hydrogène. -Workshop sur l'hydrogène WIH2'2005 -CDER, Alger 2005, p.[1-8].
4. **Bezazi, A.**, **El Mahi, A.**, **Berthelot, J.-M.**, **Bezzazi, B.** Analyse de l'endommagement des stratifiés en flexion 3-points. Influence de la séquence d'empilement. -XV^{ème} Congrès Français de Mécanique, Nancy, 2001, p.[1-6].
5. **Bezazi, A.**, **El Mahi, A.**, **Berthelot, J.-M.**, **Bezzazi, B.** Flexure fatigue behaviour of cross-ply laminates -An experimental approach. -Strength of Materials, 2003, v.35, No2, p.149-161.
6. **Kabir, M. Z.** Finite element analysis of composite pressure vessels with a load sharing metallic liner, -Composite Structures, 2000, v.49, p.247-255.
7. **Xia**, **M.**, **Takayanagi, H.**, **Kemmochi, K.** Analysis of multilayered filament -wound composite pipes under internal pressure. -Composites structures, 2001, v.53, p.483-491.
8. **Xia**, **M.**, **Takayanagi, H.**, **Kemmochi, K.** Analysis of filament-wound reinforced sandwich pipe under combined internal pressure and thermomechanical loading. -Composite structures, 2001, v.51, p.273-283.
9. **Parnas, L.**, **Katrice, N.** Design of fiber-reinforced composite pressure vessels under various loading conditions. -Composite Structures, 2002, v.58, p.83-95.

10. **Lifshitz, J.M.**, **Dayan, H.** Filament–wound pressure vessel with thick metal liner. -Composite Structures, 1995, v.32, p.313-323.
11. **Hocine, A.**, **Bezazi, A., Benamar, A.** Analysis of the influence of stacking sequence on the mechanical behaviour of composite fuel tanks. -JNC14.-Compiègne: Published by Benzaggah M.L. and Lamon J, 2005, p.641-649.
12. **Hocine A., Bezazi A., Benamar A.**. Analyse numérique d'un réservoir composite liner sous pressions. Workshop sur la Modélisation en Electrotechnique et en Mécanique MEM'05 – ENP, Alger. Algerian Journal of Technology (AJOT), 2005, special issue, p.201-206.
13. **Hocine, A., Bezazi, A.**, **Boubakar, L.**, **Benamar, A., Kondratas, A.** Multilayer tubular composite reinforced by a liner: behaviour under pressure loading simulation. -Mechanika. -Kaunas: Technologija, 2005, No5(55), p.11-19.
14. **Berthelot, J.-M.** Composite Materials.-Mechanical Behaviour and Structural Analysis.-New York: Springer, 1999.-676p.
15. **Wang, X., Zhang, Y.C., Dai, H.L**. Critical strain for a locally elliptical delamination near the surface of a cylindrical laminated shell under hydrothermal effects. -Composite Structures, 2005, v.67, p.491-499.

A. Hocine, A. Bezazi, A. Benamar, L. Boubakar,
A. Kondratas

DAUGIASLUOKSNIS VAMZDINIS KOMPOZITAS SU ĮKLOTU: ELGSENOS, VEIKIANT TERMOMECHANINEI APKROVAI, MODELIAVIMAS

R e z i u m ė

Darbe pateikta daugiasluoksnio vamzdžio (t. y. cilindrinio bako vidurinės dalies), armuoto metaliniu įklotu, įtempių ir deformacijų, veikiant termomechaninei apkrovai, analizė. Tamprios struktūros elgsenai analizuoti buvo taikomas analitinis modeliavimo metodas. Darbo tikslas – ištirti atitinkamą kompozito sluoksnių padengimo eiliškumą, kad būtų galima padidinti bako atsparumą atlaikyti didesnes termomechanines apkrovas. Buvo modeliuoti du kompozito sluoksnių uždėjimo ant įkloto eiliškumo tipai: antisimetrinis ir kvaziizotropinis. Gauti rezultatai rodo, kad dėl terminio poveikio įtempiai ir deformacijos kinta skirtingai ir priklauso nuo kompozito sluoksnių, uždėtų ant įkloto, tipo. Jautriausi temperatūriniam poveikiui yra radialiniai įtempiai ir apkrovos. Kvaziizotropinio tipo kompozito sluoksnis yra atsparesnis ir mažiau deformuojasi nei antisimetrinio tipo kompozito sluoksnis.

A. Hocine, A. Bezazi, A. Benamar, L. Boubakar,
A. Kondratas

MULTILAYER TUBULAR COMPOSITE REINFORCED BY A LINER: BEHAVIOUR UNDER THERMOMECHANICAL LOADING SIMULATION

S u m m a r y

This paper presents the investigation of elastic behaviour of a multilayer composite tube (tubular part of the cylindrical tank) reinforced by a metal liner under the thermomechanical loading using an analytical simulation. The aim of this study was to highlight the thermal effect on the stresses, strains, and displacements through the thickness in order to improve the resistance of the tank for supporting higher thermomechanical loadings. A metal liner coated with two different stacking sequence laminates, such as: the antisymmetric and the quasi-isotropic stackings are used in this simulation. The analysis of the obtained results shows that the presence of the thermal effect changes the stresses, strains, and displacements with different sensitivities and depend on the used stacking sequence. The greatest influence is recorded for radial stresses and strains. The lay-up of the quasi-isotropic laminate presents the best results in term of stresses and displacements compared to the anti-symmetric lay-up one.

А. Хоцине, А. Безази, А. Бэнамар, Л. Боубакар,
А. Кондратас

МНОГОСЛОЙНЫЙ ТРУБЧАТЫЙ КОМПОЗИТ УСИЛЕННЫЙ ВКЛАДЫШЕМ: МОДЕЛИРОВАНИЕ ПОВЕДЕНИЯ ПОД ТЕРМОМЕХАНИЧЕСКОЙ НАГРУЗКОЙ

Р е з ю м е

В работе представлен анализ напряжений и деформаций многослойного трубчатого композита (трубчатой части цилиндрического бака), усиленного металлическим вкладышем под воздействием термомеханической нагрузки. Для анализа упругого поведения структуры под давлением использован аналитический метод моделирования. Целью этого исследования является определение соответствующей последовательности нанесения слоев композита, чтобы увеличить способность бака выдерживать более высокие термомеханические нагрузки. Для этого моделирования были применены два способа последовательности нанесения слоев на металлический вкладыш: антисимметричный и квазиизотропный. Анализ полученных результатов показывает, что вследствие термического воздействия изменяются напряжения и перемещения по разному для композитов с разными способами укладки слоев. Наибольшее влияние изменения температуры отмечено на радиальные напряжения и нагрузки. Квазиизотропный способ укладки слоев показал лучшие результаты в виде выдерживаемых нагрузок и перемещений по сравнению с антисимметричным способом укладки слоев композита.

Received August 15, 2005